Broadband and Low-Profile Microstrip Antenna Using Strip-Slot Hybrid Structure

Wangyu Sun, Yue Li, *Senior Member, IEEE*, Zhijun Zhang, *Fellow, IEEE*, and Zhenghe Feng, *Fellow, IEEE*

***Abstract*—In this letter, a low-profile microstrip antenna with strip-slot hybrid structure is proposed to enhance the bandwidth up to 41% within a height of $0.06\lambda_0$ (λ_0 is the center operating wavelength in free space). The proposed antenna consists of four strips, which are separated by three narrow slots. By controlling the dimensions of the strips and the slots, dual modes, i.e., TM_{10} mode and antiphase TM_{20} mode, are excited and coupled to increase the operating bandwidth. The strip-slot hybrid structure can be excited with optimized impedance matching using an aperture-coupled Y-shaped feeding microstrip line. A prototype of the proposed antenna is constructed and tested. Experimental results show an impedance bandwidth of 41% for the reflection coefficient less than −10 dB, achieving an obvious improvement of operating bandwidth with a low profile of $0.06\lambda_0$.**

***Index Terms*—Antenna feeds, broadband antennas, microstrip antennas.**

I. Introduction

With the rapid development of wireless communications, the microstrip antenna has been generally applied in many communication devices because of its obvious advantages, e.g., low manufacturing cost, easy fabrication, and low profile [1]. However, the main limitation of traditional microstrip antennas is the narrow impedance bandwidth (typically less than 3% with reflection coefficient lower than −10 dB). For various wideband wireless communication services, several bandwidth enhancement techniques based on microstrip antennas have been studied and verified [2]–[6]. The use of six rectangular strips in [2] realizes a larger impedance bandwidth of 6%. A broadband circular microstrip antenna achieves a fractional bandwidth of 13.6% using diamond-shaped slot in [3]. By embedding a U-shaped slot within the rectangular patch, the impedance bandwidth is achieved over 20% [4]. A broadband E-shaped microstrip antenna is presented in [5] to achieve an excellent bandwidth of 30.3%. A Y-shaped stub proximity-coupled V-slot microstrip antenna presented in [6] shows an enhanced impedance bandwidth of 21%. As another feasible solution to improve the bandwidth of microstrip antennas, planar multilayer configuration is used in [7] with 25% bandwidth. With the similar strategy, aperture-coupled stacked microstrip antennas are achieved with the bandwidth over 20% for millimeter-wave applications [8] and over 25% on a low-temperature cofired ceramic substrate [9]. Based on double-Y-shaped aperture-coupling technique, a 10 dB impedance bandwidth of 71% (3.28–6.76 GHz) is achieved in [10] with the size of $28 \times 28 \times 15\,\text{mm}^3$. Recently, the concept of metamaterial-inspired microstrip antennas is investigated to achieve wide bandwidth, e.g., mushroom [11] and grid-slotted [12] structures with 25% and 28% impedance bandwidth, respectively.

In this letter, with the purposed to improve the impedance bandwidth of traditional microstrip antennas, a low-profile wideband microstrip antenna with strip-slot hybrid structure is proposed. The strip-slot hybrid structure is composed of four strips and three narrow slots. A Y-shaped microstrip feeding line is introduced to feed this antenna through a coupling aperture on the ground. By optimizing the sizes of the strips and the slots, TM_{10} mode and antiphase TM_{20} mode are excited, and coupled together to enhance the impedance bandwidth up to 41% with a low profile of $0.06\lambda_0$. The proposed strip-slot hybrid structure is systematically simulated using the full-wave simulation software of High Frequency Structure Simulator and validated experimentally.

II. Design Procedure

A. Antenna Structure and Configuration

The overall geometry of the proposed microstrip antenna with strip-slot hybrid structure is illustrated in Fig. 1. This antenna has a three-layer structure and Fig. 1(a) shows the perspective view of the layered structure. There are three metallic layers: radiating patch on the top layer; ground plane with coupling aperture on the middle layer; and Y-shaped feeding structure on the bottom layer. Between the three metallic layers, there are two layers dielectrics with the same relative permittivity ε_0 of 3.38 and loss tangent $\tan\delta$ of 0.0027. The overall volume of the upper dielectric is $G_W \times G_L \times h$, and the overall dimension of the lower dielectric is $G_W \times G_L \times h_0$.

In Fig. 1(b), we can see that the radiating patch has a strip-slot hybrid structure, which is composed of four identical strips arranged periodically with three narrow slots between each two adjacent strips. The length and width of each strip are W_p and w, and the slots are with the same width of g. In Fig. 1(c)

Manuscript received September 1, 2017; accepted October 13, 2017. Date of publication October 16, 2017; date of current version November 20, 2017. This work was supported in part by the National Natural Science Foundation of China 61771280, in part by the China Postdoctoral Science Foundation funded project 2015T80084, and in part by the the National Basic Research Program of China under Grant 2013CB329002. *(Corresponding author: Yue Li.)*

The authors are with the Department of Electronic Engineering, Tsinghua University, Beijing 100084, China (e-mail: sunwy16@mails.tsinghua.edu.cn; lyee@tsinghua.edu.cn; zjzh@tsinghua.edu.cn; fzh-dee@tsinghua.edu.cn).

Color versions of one or more of the figures in this letter are available online at http://ieeexplore.ieee.org.

Digital Object Identifier 10.1109/LAWP.2017.2763987

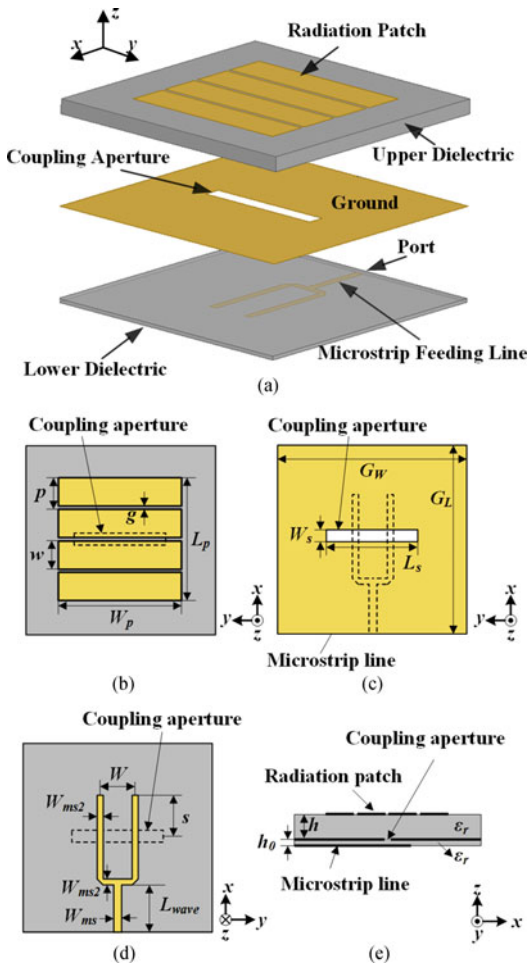

Fig. 1. Geometry and dimensions of the proposed antenna: (a) Perspective view of the layered structure, (b) top layer of the radiating patch with strip-slot hybrid structure, (c) middle layer of the ground with the coupling aperture, (d) bottom layer of the Y-shaped feeding microstrip line. (e) Side view of the overall structure.

TABLE I
OPTIMIZED DIMENSIONS OF THE PROPOSED ANTENNA (UNIT: mm)

p	g	W_p	G_L	G_W	W_s	L_s	w
10	1.1	40	60	60	3.8	29	8.9
W	s	W_{ms}	W_{ms2}	L_{wave}	h_0	h	
8	10	1.85	1.75	15	0.813	3.25	

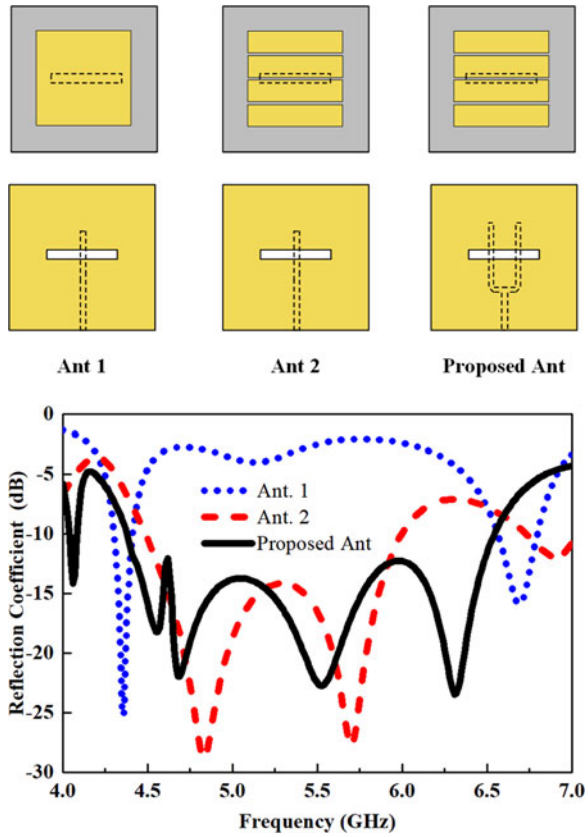

Fig. 2. Geometries and simulated reflection coefficients of the three antennas with different radiating patches and feeding structures.

and (d), the coupling aperture is cut on the ground plane, and placed underneath and parallel to the center slot on the top layer. The dimensions of the coupling aperture are $L_s \times W_s$. The 50 Ω Y-shaped microstrip feeding structure is printed on the bottom layer of the lower dielectric, and it is symmetrical with respect to the x-axis. This microstrip feeding line is composed of two sections: the straight section of width W_{ms} and two arm sections of equal width W_{ms2}. The length of the straight section is L_{wave}. The end of the arm section has a vertical distance of s away from the y-axis. The distance between the two arms is W. By optimizing the dimensions of the strip-slot hybrid structure and Y-shaped feeding structure, the impedance bandwidth of this antenna can be improved obviously. The side view of the proposed antenna is shown in Fig. 1(e), and all the optimized dimensions of the proposed antenna are tabulated in Table I.

B. Structure Evolution

With the purpose of increasing the impedance bandwidth of microstrip antenna, we modify the structure of the radiating patch and the microstrip feeding line based on the traditional configuration. The geometric evolution process of the proposed antenna is shown in Fig. 2. First, the Ant 1 is composed of a square radiating patch and a straight microstrip feeding line. Then, the Ant 2 applies the strip-slot hybrid structure as the radiating patch, which is also fed by a straight microstrip line. Finally, the proposed antenna uses the strip-slot hybrid radiating structure and the Y-shaped microstrip feeding structure together. The radiating patches of these three antennas are with the same size and excited by these microstrip lines through coupling apertures cut on the ground plane. The simulated reflection coefficients are shown in Fig. 2. The dimensions of the coupling apertures and microstrip feeding lines are optimized to good impedance matching. As we can see, the simulated bandwidth of the reflection coefficient less than −10 dB is 4.3–4.43 GHz or 3% for the Ant 1, and is 4.49–6 GHz or 28.8% for the Ant 2. The enhancement of the bandwidth is due to the introduction of the strip-slot hybrid structure, which excites an extra operating mode, i.e., antiphase TM_{20} mode. The TM_{10} mode

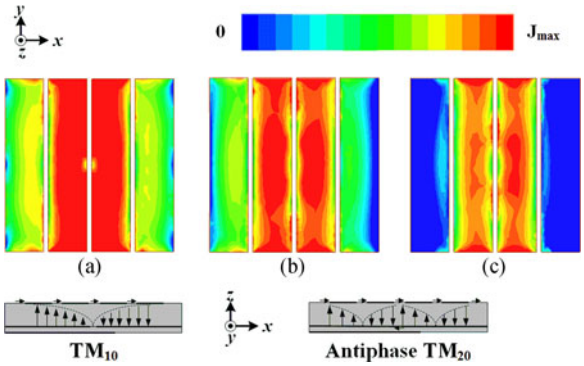

Fig. 3. Current distributions and operating modes of the proposed antenna at different resonances: (a) 4.7 GHz. (b) 5.5 GHz. (c) 6.3 GHz.

and antiphase TM_{20} mode are coupled together to increase the operating bandwidth. As for the proposed antenna, it achieves an impedance bandwidth of 4.37–6.55 GHz or 39.9% for the reflection coefficients less than −10 dB. Compared with the Ant 2, no new mode is excited by the proposed antenna. The added resonant at 6.3 GHz is introduced from the impedance matching by the Y-shaped feeding structure, with 11% incensement of bandwidth. That is to say, this modified feeding structure increases the degree of freedom for optimizing and improves the impedance matching of the proposed antenna. A parasitic mode appears at 4.1 GHz with a different broadside radiation pattern, and not included in the bandwidth of 4.37–6.55 GHz.

C. Operating Mechanism

To understand the operating mechanism of the proposed antenna, the snapshots of the current distributions at three resonances are shown in Fig. 3. These three resonances appear at the frequencies of 4.7, 5.5, and 6.3 GHz, respectively. Except for the radiation of the slots between adjacent strips, the current distributions at 4.7 GHz are similar to the TM_{10} mode excited in the traditional microstrip antenna. On the other hand, the current distributions at 5.5 and 6.3 GHz are almost the same, and the resonant mode resembles the antiphase TM_{20} mode. Due to the radiation of the coupling aperture and the strip-slot hybrid structure, the opposite sides of the center slot have the antiparallel E-fields. The theoretical analysis and calculation of the antiphase TM_{20} mode can be carried out by using the transmission-line model [12]. By coupling the two resonant modes together, an enhanced bandwidth of the proposed antenna can be realized.

III. Prototype and Measurements

Based on the optimized dimensions in Table I, the proposed complete structure of the antenna is fabricated and measured to validate the broadband performance. Fig. 4(a)–(c) shows the photographs of the fabricated antenna (top view, GND layer and bottom view). The Agilent E5071B vector network analyzer is used to measure the reflection coefficient, and the ETS-LindgrenAMS8500 anechoic chamber is used to test the radiation performance of the proposed antenna.

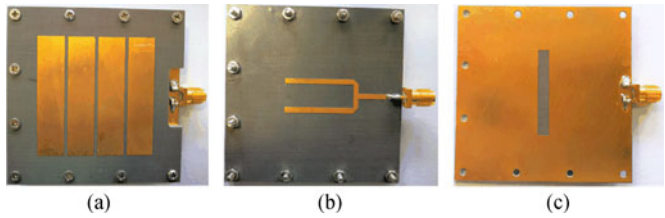

Fig. 4. Photographs of the fabricated antenna: (a) top layer of the radiating patch with strip-slot hybrid structure, (b) Y-shaped microstrip feeding line in the bottom layer, and (c) middle layer of the ground with the coupling aperture.

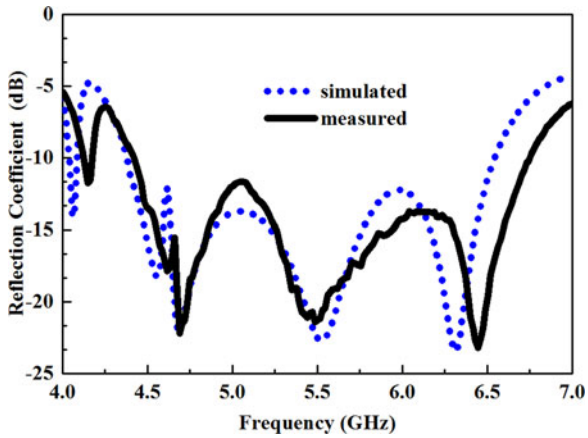

Fig. 5. Simulated and measured reflection coefficients of the proposed microstrip antenna.

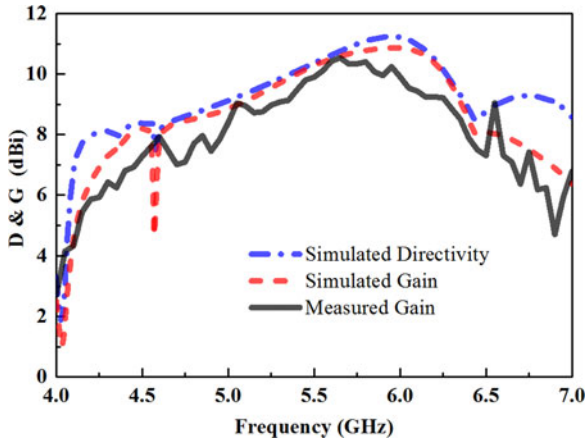

Fig. 6. Simulated directivity, simulated gain and measured gain of the proposed microstrip antenna.

The simulated and measured reflection coefficients are illustrated in Fig. 5. The simulated bandwidth of the reflection coefficient less than −10 dB is 4.37–6.55 GHz or 39.9%, and the measured bandwidth of the reflection coefficient less than −10 dB is 4.42–6.76 GHz or 41.1%. The simulated and measured results are in good agreement, and the slight difference is mainly caused by manufacturing and measurement error. In Fig. 6, we show the simulated directivity and simulated and measured gain of the proposed antenna. In the whole operating bandwidth

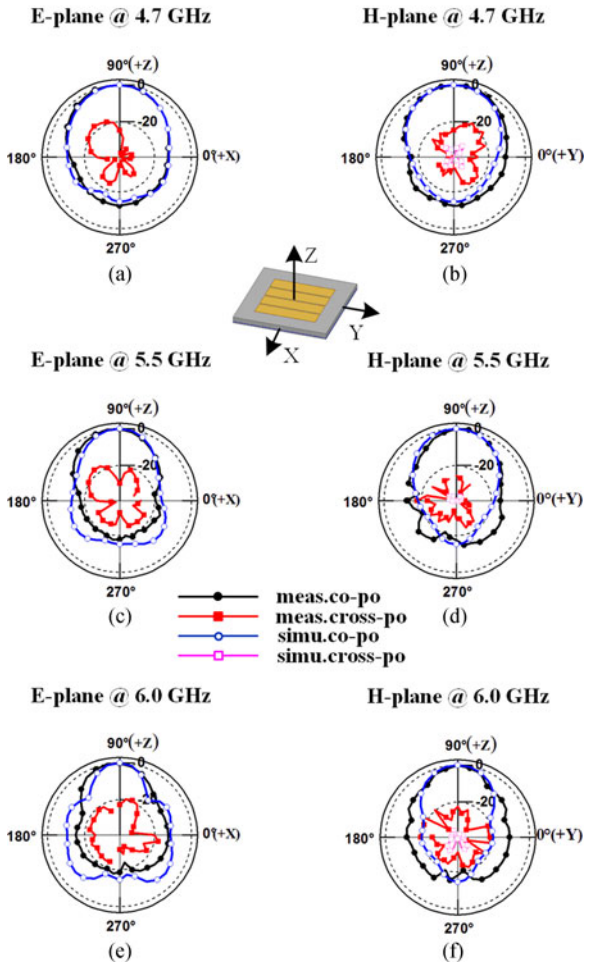

Fig. 7. Simulated and measured normalized radiating patterns of the proposed microstrip antenna at 4.7, 5.5 and 6 GHz in *E*-plane and *H*-plane.

(4.37–6.55 GHz), the simulated gain ranges from 7.52 to 10.89 dBi and the antenna efficiency is above 85%. In the whole operating bandwidth (4.42–6.76 GHz), the measured gain ranges from 6.82 to 10.56 dBi and the efficiency is higher than 78%.

Fig. 7 shows the simulated and measured normalized radiating patterns of the proposed antenna at 4.7, 5.5, and 6.0 GHz. It is observed that the simulated and measured copolarization patterns agree with each other very well in both *E*-plane and *H*-plane. The deviations may be caused by the measurement errors of the anechoic chamber. Besides, the cross polarization of the proposed antenna is also measured and presented in Fig. 7. The simulated cross-polarization levels are below -50 dB in *E*-plane and -35 dB in *H*-plane compared with the main polarization levels. Meanwhile, the cross-polarization levels of about -20 dB in *E*-plane and -19 dB in *H*-plane lower than the copolarization levels can be observed in the measured radiation patterns. The measured radiation patterns show a good broadside radiating performance and remain stable over the whole operating bandwidth.

TABLE II
COMPARISON OF BANDWIDTH FOR VARIOUS MICROSTRIP ANTENNAS (λ_0 IS THE CENTER OPERATING WAVELENGTH IN FREE SPACE)

Antenna	Methods	Profile	BW
Ref. [12]	Metamaterial-based	$0.06\,\lambda_0$	28%
Ref. [13]	Shorting Pins-loaded	$0.032\,\lambda_0$	15.2%
Proposed	Strip-slotted	$0.06\,\lambda_0$	41.1%

IV. CONCLUSION

In this letter, to increase the bandwidth of the traditional microstrip antenna, a broadband microstrip antenna with modified radiating patch and feeding structure is proposed. The square radiating patch is replaced by a strip-slot hybrid structure, which contains four strips and three narrow slots. Modified from the straight microstrip feeding line, a Y-shaped microstrip line is applied to improve the matching performance. By coupling the two resonant modes together through proper impedance matching, the bandwidth of the proposed antenna can be broadened greatly. Compared with the similar antennas [12], [13] in Table II, the proposed antenna achieves a wider bandwidth of 41.1% with a low profile of $0.06\,\lambda_0$. Due to the characteristics of broad band and low profile, the proposed antenna using strip-slot hybrid structure is with the potential in modern wireless communication systems.

REFERENCES

[1] D. M. Pozar, "Microstrip antennas," *Proc. IEEE*, vol. 80, no. 1, pp. 79–91, Jan. 1992.
[2] C. K. Aanandan and K. G. Nair, "Compact broadband microstrip antenna," *Electron. Lett.*, vol. 22, pp. 1064–1065, 1986.
[3] G. D. Bhatnagar, J. S. Saini, V. K. Saxena, and L. M. Joshi, "Design of broadband Circular patch microstrip antenna with diamond shape slot," *Indian J. Radio Space Phys.*, vol. 40, pp. 275–281, Oct. 2011.
[4] T. Huynh and K. F. Lee, "Single-layer single-patch wideband microstrip antenna," *Electron. Lett.*, vol. 31, no. 16, pp. 1310–1312, Aug. 1995.
[5] F. Yang, X.-X. Zhang, X. Ye, and Y. Rahmat-Samii, "Wide-band E-shaped patch antennas for wireless communications," *IEEE Trans. Antennas Propag.*, vol. 49, no. 7, pp. 1094–1100, Jul. 2001.
[6] S. Qu and Q. Xue, "A Y-shaped stub proximity coupled V-slot microstrip patch antenna," *IEEE Antennas Wireless Propag. Lett.*, vol. 6, pp. 40–42, 2007.
[7] G. Kumar and K. P. Ray, "Stacked gap-coupled multi-resonator rectangular microstrip antennas," *IEEE Antennas Propag. Symp. Dig.*, vol. 3, pp. 514–517, Jul. 2001.
[8] F. Croq and D. M. Pozar, "Millimeter wave design of wide-band aperture-coupled stacked microstrip antennas," *IEEE Trans. Antennas Propog.*, vol. 39, no. 12, pp. 1770–1776, Dec. 1991.
[9] C. Kuo-Sheng, C. Ho-Ting, and L. Jia-An, "Design of LTCC wide-band patch antenna for LMDS band applications," *IEEE Antennas Wireless Propag. Lett.*, vol. 9, pp. 1111–1114, 2010.
[10] J. Wei, X. Jiang, and L. Peng, "Ultrawideband and high-gain circularly polarized antenna with double-Y-shape slot," *IEEE Antennas Wireless Propag. Lett.*, vol. 16, pp. 1508–1511, 2017.
[11] W. Liu, Z. N. Chen, and X. Qing, "Metamaterial-based low-profile broadband mushroom antenna," *IEEE Trans. Antennas Propag.*, vol. 62, no. 3, pp. 1165–1172, Mar. 2014.
[12] W. Liu, Z. N. Chen, and X. M. Qing, "Metamaterial-based low-profile broadband aperture coupled grid-slotted patch antenna," *IEEE Trans. Antennas Propag.*, vol. 63, no. 7, pp. 3325–3329, Jul. 2015.
[13] N.-W. Liu, L. Zhu, W.-W. Choi, and J.-D. Zhang, "A low-profile aperture-coupled microstrip antenna with enhanced bandwidth under dual resonance," *IEEE Trans. Antennas Propag.*, vol. 65, no. 3, pp. 1055–1062, Mar. 2017.